# Nonvolatile memories using deep traps formed in $Al_2O_3$ by metal ion implantation

Min Choul Kim,[1] Seung Hui Hong,[1] Hye Ryong Kim,[1] Sung Kim,[1] Suk-Ho Choi,[1,a)]
R. G. Elliman,[2] and S. P. Russo[3]
[1]*Department of Applied Physics, College of Applied Sciences, Kyung Hee University, Yongin 440-701, Republic of Korea*
[2]*Department of Electronic Materials Engineering, Research School of Physical Sciences and Engineering, Australian National University, Canberra, Australian Capital Territory 0200, Australia*
[3]*Department of Applied Physics, School of Applied Sciences, RMIT University, Melbourne, Victoria 3000, Australia*

(Received 7 November 2008; accepted 17 February 2009; published online 19 March 2009)

We demonstrate the feasibility of an approach to nonvolatile memory (NVM) that exploits charge trapping at deep-energy levels formed in $Al_2O_3$ by metal doping. Our calculations show that V and Nb are expected to form such deep energy levels in the band gap of $Al_2O_3$. To demonstrate the effectiveness of this approach these metal ions were ion-implanted into test structures based on an $Al_2O_3$ trapping layer. Several structural analysis techniques and photocurrent spectroscopy show that the doped metal ions are located close to the $Al_2O_3/SiO_2$ interface and exhibit characteristics consistent with some of the deep levels predicted in calculations. The resulting test devices are shown to exhibit promising NVM characteristics. © *2009 American Institute of Physics*. [DOI: 10.1063/1.3097799]

To overcome the limitations of conventional nonvolatile memory (NVM) devices based on floating-gate transistors with poly-Si gates, several discrete charge-trap structures have been studied including semiconductor and metal nanocrystals (NCs)[1,2] and nitride traps.[3] However, the trap density of Si-NC-based NVMs is typically only in the range of $10^{11}$–$10^{12}$ $cm^{-2}$,[4,5] insufficient to ensure reliable data storage in high-density (HD) NVMs (Ref. 6), and insufficient to provide a secure memory widow for multilevel (ML) memories. Metal NCs/nanodots (NDs) offer several advantages compared to their semiconductor counterparts[7] but their thermal stability needs to be improved for reliable NVM device fabrication. Ideally, the tunnel oxide in NVMs should only be a few nanometers thick, especially for the ML programming, but such thin oxides typically reduce the retention time due to charge leakage. In order to overcome this problem, dielectrics such as $Al_2O_3$ (Ref. 8) and SiN,[9] layered tunnel barriers,[10] and hybrid trapping layer with NDs and SiN (Ref. 11) have been investigated as alternative materials/structures for advanced NVMs. Recently, nitride-trap-based memory cells[3,12] have received particular attention for HD-ML flash memory applications. However, it is difficult to control the density and the energy of the naturally formed nitride traps. Recently, studies have shown the formation of the band gap states in transition-metal-doped dielectrics.[13,14] This letter demonstrates the feasibility of an approach to NVM that exploits charge trapping at deep-energy levels formed in $Al_2O_3$ by metal doping.

For the fabrication of metal-oxide-semiconductor (MOS) memory cells, a 5 nm $SiO_2$ layer was first grown on *p*-type (100) Si wafer by conventional thermal oxidation. A 40 nm $Al_2O_3$ layer was then grown on top of the $SiO_2$ layer by atomic layer deposition. These $Si/SiO_2/Al_2O_3$ structures were then implanted at room temperature (RT) with V and Nb ions of two different energies: 50/70 and 80/100 keV, respectively, to nominal fluences in the range from $10^{12}$ to $10^{16}$ $cm^{-2}$. In order to assess the contribution of radiation damage, control samples were implanted with AlO ions of 25 keV to nominal fluences of $10^{14}$ and $10^{15}$ $cm^{-2}$. The samples were subsequently annealed in a rapid thermal annealing apparatus at a temperature of 800 °C for 1 min under an $N_2$ ambient. The high- and low-energy implanted samples will be referred to as HE-V (or -Nb) and LE-V (or -Nb) memory cells, respectively, for each metal ion. The peak excess V or Nb concentration for these implants was calculated from TRIM simulation to be around 3 at. % for the highest fluence.[15]

Photoconductivity (PC) spectra were measured using a coplanar, two-probe geometry with Al electrodes of 4 mm length and 2 mm separation to characterize the impurity energy levels in the band gap. The PC spectra were measured in a $LN_2$ refrigerator by using a xenon lamp as the light source under a bias of 1 V, which belongs to the linear range of *I-V* characteristics. The power density of the incident light on the sample surface was about 20–290 $mW/cm^2$ depending on photon energy and was corrected for uniform distribution in the measurement range of 2–5 eV. Al electrodes with a diameter of 100 $\mu$m were deposited on the samples in vacuum for capacitance-voltage (*C-V*) measurements of MOS capacitors. High-frequency *C-V* measurements were carried out by using an Agilent 4284A *C-V* meter with a frequency of 1 MHz and a modulation signal amplitude of 100 mV. The programming and erasing operations were carried out with an Agilent 8114A pulse generator together with the Agilent 4284A.

TRIM simulations of HE-V cells predict a peak dopant concentration close to the $Al_2O_3/SiO_2$ interface, ignoring sputtering effects, but the final dopant distribution is affected by annealing. For the HE-V cell implanted to a fluence of $10^{14}$ $cm^{-2}$, two major V peaks are observed in the secondary ion mass spectroscopy (SIMS) spectra after annealing, one at ~36 nm and one at ~47 nm from the surface.[16] A deeper peak in the Si substrate is likely due to trapping of V at

a)Author to whom correspondence should be addressed. Electronic mail: sukho@khu.ac.kr.

 

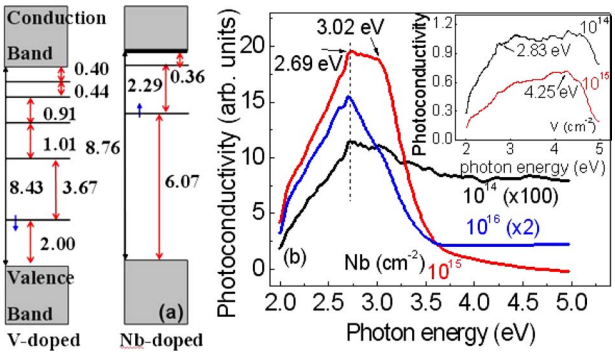


FIG. 1. (Color online) (a) Schematic diagram showing the calculated impurity energy levels for V and Nb doped $Al_2O_3$. (b) Photoconductivity spectra of HE memory cells containing V or Nb ions.

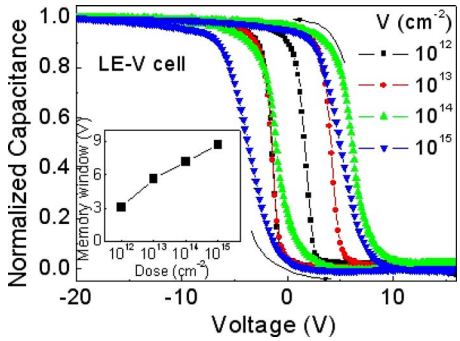


FIG. 2. (Color online) *C-V* hysteresis loops of LE memory cells containing V ions of $10^{12}$–$10^{15}$ cm$^{-2}$ fluences. The inset shows memory window as a function of fluence.

end-of-range defects. The data suggest that V atoms have accumulated on the Si-side of the $Si/SiO_2$ interface during annealing. This is confirmed by transmission electron microscopy (TEM) analysis which shows the presence of V-precipitates at this location. Similar SIMS profiles are observed for the LE-V cell implanted with a fluence of $10^{14}$ V cm$^{-2}$, except that the concentration of V atoms remaining in the region of the projected range is relatively larger due to the lower implantation energy.[16] These distributions were further confirmed by scanning-mode TEM (STEM) and x-ray photoelectron spectroscopy (XPS).[16]

Periodic spin-unrestricted density functional theory calculations using the B3LYP functional[17] were performed in order to predict the energies of the defect levels introduced by V and Nb doping of $\alpha$-$Al_2O_3$. The predicted band gap for the bulk (undoped) $\alpha$-$Al_2O_3$ lattice using B3LYP was 8.43 eV, which is in excellent agreement with experimental results.[18] V and Nb atoms were then placed substitutionally on Al sites in a $2\times2\times1$ $\alpha$-$Al_2O_3$ supercell lattice and allowed to relax. The atomic concentration of dopant atoms in each case was ~0.83 at. % (1 in 120 atoms). Once relaxed, the electronic density of states (eDOS) for each structure was calculated.[16] Figure 1(a) gives the energy level diagram of the states introduced into the band gap by V and Nb doping (compared to bulk $\alpha$-$Al_2O_3$) as determined from the eDOS results. The eDOS data for V doping predict that five defect states are introduced into the gap and that these states may act as electron-traps. The defect states occur at energies of 0.40, 0.84, 1.75, 2.76, and 6.43 eV below the conduction band minimum (CBM) for the V-doped lattice. The lowest defect state at 6.43 eV below the CBM is partially occupied, while the higher energy defect states are unoccupied. The predicted band gap for the V doped lattice is 8.43 eV, which is the same as in the undoped lattice. For the Nb doped lattice, two distinct defect (electron-trap) states are introduced into the band gap at energies of 0.36 and 2.65 eV below the CBM. The lowest defect state (2.65 eV below the CBM) is the only occupied defect state. There is also a small defect peak, which is ~35 meV below the CBM at $T=0$ K. This is represented in Fig. 1(a) by a thick black line just below the CBM edge. The B3LYP calculations predict that Nb doping increases the band gap of the lattice to 8.76 eV. Similar calculations were also done for Ta doped $Al_2O_3$, and the defect states were found to be relatively shallower.[16]

Figure 1(b) shows PC spectra at 80 K for several HE-V and HE-Nb cells. The PC spectra of the HE-Nb cells are peaked at around 2.69 eV, almost irrespective of fluence. This peak could be attributed to the defect level at 2.65 below CBM of Nb doped $Al_2O_3$, as shown in Fig. 1(a). Previously, a defect level at 2.3 eV below conduction band has been found in Nb-doped $Al_2O_3$ by x-ray absorption spectroscopy.[13] The peak observed at around 3.02 eV for the HE-Nb cell with a fluence of $10^{15}$ cm$^{-2}$ does not exist in the calculated results, so this peak is likely due to a natural defect in $Al_2O_3$. The HE-V cells show less-featured PC spectra, possibly resulting from the existence of multiple defect levels in the band gap of V doped $Al_2O_3$, as shown in Fig. 1(a). The PC peak at around 2.83 eV is approximately consistent with the calculated defect level at 2.76 eV below CBM. The peak observed at around 4.25 eV for the HE-V cell with a fluence of $10^{15}$ cm$^{-2}$ also seems to originate from a natural defect in $Al_2O_3$. The PC spectra of control samples with $AlO^-$ ions of $10^{14}$ and $10^{15}$ cm$^{-2}$ fluences are peaked at energies of 2.13/4.10 and 2.13/3.86 eV, respectively, which are very different from those of the metal-doped $Al_2O_3$. These results suggest that the defect levels observed in the band gap of the metal-doped $Al_2O_3$ are formed by doping, not by the radiation damage.

Figure 2 shows *C-V* hysteresis loops of LE-V cells with different implant fluences under applied voltages of ±20 V. All samples show counterclockwise *C-V* hysteresis loops, indicating electron injection from the Si substrate to the charge-trapping layer containing V atoms. The hysteresis width or the memory window increases with increasing the implant fluence due to the increase in charge-trapping states, as shown in the inset. The amount of charge stored in the traps can be estimated by the relation $Q=C\Delta V_{MW}$, where $C$ is the capacitance density and $V_{MW}$ is the memory window.[19] In this work, $C$ and $\Delta V_{MW}$ are about $2.29\times10^{-7}$ F cm$^{-2}$ (capacitance=18 pF, contact area=$\pi\times50\times50$ $\mu$m$^2$) and 9 V, respectively, for a typical LE-V cell with a fluence of $1\times10^{15}$ cm$^{-2}$. Thus, the electron density stored in the traps is estimated as $1.3\times10^{13}$ cm$^{-2}$, which is comparable to the trap density of $Si/SiO_2/SiN/SiO_2$/poly Si memory cells.[20] Significantly, *C-V* hysteresis loops were also measured for Ru and Ta implanted $Al_2O_3$.[16] However, these samples exhibited only small *C-V* hysteresis effects compared to V and Nb doped $Al_2O_3$, possibly due to shallower trap levels, as shown in the calculations. This reduced hysteresis further suggests that the effects observed for V and Nb are impurity-related and not due to radiation damage or interface defects produced by ion implantation.

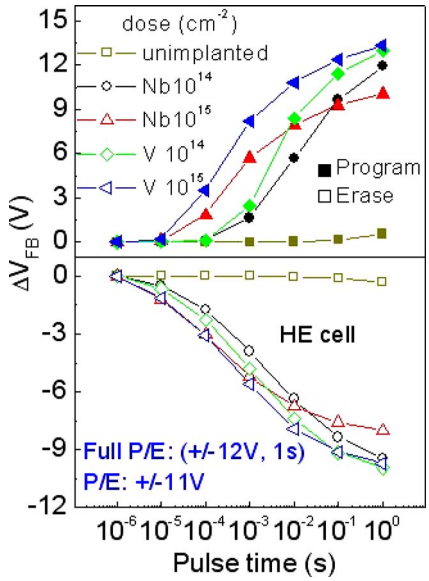


FIG. 3. (Color online) P/E characteristics of HE memory cells containing V and Nb ions of $10^{14}$ and $10^{15}$ $cm^{-2}$ fluences.

The program/erase (P/E) properties based on the Fowler–Nordheim tunneling scheme were obtained by measuring the flat-band voltage shift ($\Delta V_{FB}$) in *C-V* curves under a voltage pulse. Figure 3 shows the P/E characteristics for HE cells implanted with V and Nb. The fully programmed and fully erased states are defined as those programmed by a pulse of (+12 V, 1*s*) and erased by a pulse of (−12 V, 1*s*), respectively. The P/E speeds of the higher-fluence samples are faster over most of the time range and also show faster saturation. At the same fluence, the P/E speeds of the HE-V cell are higher than those of the HE-Nb cell. The LE cells show similar behaviors but with a clearer dependence of the erase speeds on the doping element and concentration.[16] Figure 4 shows retention characteristics of HE cells with a fluence of $10^{14}$ $cm^{-2}$ at RT. The programming was performed at +11 V during 5 ms, and the erasing at −11 V during 10 ms. The $\Delta V_{FB}$'s at the P/E states of the HE cells remain almost unchanged with time, showing very little charge transfer during the retention measurement. The expected charge loss after ten years is ~26% and ~19% for the HE-V and HE-Nb cells, respectively, which meets the retention requirement for commercial NVMs. In contrast, the charge losses are 38% and 39% for the LE-V cells with fluences of $10^{14}$ and $10^{15}$ $cm^{-2}$, respectively.[16] These results indicate that the charge loss rate is closely related to the distribution

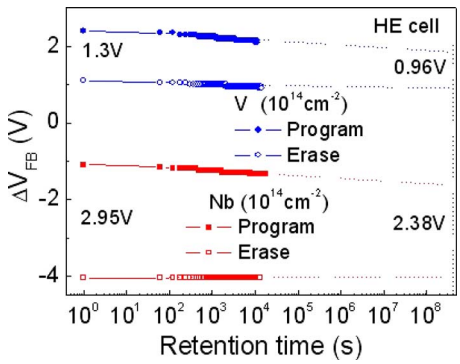


FIG. 4. (Color online) Retention characteristics of HE memory cells containing V and Nb ions of $10^{14}$ $cm^{-2}$ fluence.

of the doped elements with respect to the $Al_2O_3/SiO_2$ interface. This may also mean that the charge leakage into the metal contact is more dominant than that into the Si substrate during the retention period for the LE cells because the doped elements are distributed closer to the metal contact. On the other hand, the HE and LE cells all show excellent retention properties during erasing.

In summary, a method for fabricating NVMs was proposed based on deep-energy impurity levels formed in $Al_2O_3$ by metal doping. As V and Nb were expected to form deep energy levels in the band gap of $Al_2O_3$, these metal ions were chosen for initial tests. The STEM, SIMS, XPS, and PC data showed that the doped metal ions were well located very close to the $Al_2O_3/SiO_2$ interface and exhibited characteristics consistent with some of the deep levels predicted in calculations. The MOS memory cells containing the metal-doped $Al_2O_3$ layer showed promising NVM properties including P/E speeds and retention time.

This work was supported by the Korea Science and Engineering Foundation (KOSEF) grant funded by the Korea government (MOST) (Grant No. R01-2007-000-20142-0). M.C.K. acknowledges a support from the Kyung Hee University Graduate School Scholarship for Outstanding Research Papers in the second semester, 2007.

[1]C. J. Park, K. H. Cho, W.-C. Yang, H. Y. Cho, S.-H. Choi, R. G. Elliman, J. H. Han, and C. Kim, Appl. Phys. Lett. **88**, 071916 (2006).
[2]S. K. Samanta, W. J. Yoo, G. Samudra, E. S. Tok, L. K. Bera, and N. Balasubramanian, Appl. Phys. Lett. **87**, 113110 (2005).
[3]Y. N. Tan, W. K. Chim, W. K. Choi, M. S. Joo, T. H. Ng, and B. J. Cho, Tech. Dig. - Int. Electron Devices Meet. **2004**, 889.
[4]S. Lombardo, B. De Salvo, C. Gerardi, and T. Baron, Microelectron. Eng. **72**, 388 (2004).
[5]J. De Blauwe, M. Ostraat, M. L. Green, G. Weber, T. Sorsch, A. Kerber, F. Klemens, R. Cirelli, E. Ferry, J. L. Grazul, F. Baumann, Y. Kim, W. Mansfield, J. Bude, J. T. C. Lee, S. J. Hillenius, R. C. Flagan, and H. A. Atwater, Tech. Dig. - Int. Electron Devices Meet. **2000**, 683.
[6]H. Silva, M. K. Kim, U. Avic, A. Kumar, and S. Tiwari, MRS Bull. **29**, 845 (2004).
[7]Z. Liu, C. Lee, V. Narayanan, G. Pei, and E. C. Kan, IEEE Trans. Electron Devices **49**, 1606 (2002).
[8]C. H. Lee, S. H. Hur, Y. C. Shin, J. H. Choi, D. G. Park, and K. Kim, Appl. Phys. Lett. **86**, 152908 (2005).
[9]M. She, H. Takeuchi, and T. J. King, IEEE Electron Device Lett. **24**, 309 (2003).
[10]H. T. Lue, S. Y. Wang, E. K. Lai, Y. H. Shih, S. C. Lai, L. W. Yang, K. C. Chen, J. Ku, K. Y. Hsieh, R. Liu, and C. Y. Lu, Tech. Dig. - Int. Electron Devices Meet. **2005**, 547.
[11]S. Choi, H. Yang, M. Chang, S. Baek, H. Hwang, S. Jeon, J. Kim, and C. Kim, Appl. Phys. Lett. **86**, 251901 (2005).
[12]C. Kang, J. Choi, J. Sim, C. Lee, Y. Shin, J. Park, J. Sel, S. Jeon, Y. Park, and K. Kim, Proceedings of the 45th IEEE International Reliability Physics Symposium, 2007 (unpublished), p. 167.
[13]R. Jung, J.-C. Lee, Y.-W. So, T.-W. Noh, S.-J. Oh, J.-C. Lee, and H.-J. Shin, Appl. Phys. Lett. **83**, 5226 (2003).
[14]D. Morris, Y. Dou, J. Rebane, C. E. J. Mitchell, R. G. Egdell, D. S. L. Law, A. Vittadini, and M. Casarin, Phys. Rev. B **61**, 13445 (2000).
[15]J. P. Biersack and L. G. Haggmark, Nucl. Instrum. Methods **174**, 257 (1980).
[16]See EPAPS Document No. E-APPLAB-94-008911 for further theoretical methods/data and experimental data. For more information on EPAPS, see http://www.aip.org/pubservs/epaps.html.
[17]R. Dovesi, B. Civalleri, R. Orlando, C. Roetti, and V. Saunders, Rev. Comput. Chem. **21**, 1 (2005).
[18]R. H. French, J. Am. Ceram. Soc. **73**, 477 (1990).
[19]Z. Tan, S. K. Samanta, W. J. Yoo, and S. Lee, Appl. Phys. Lett. **86**, 013107 (2005).
[20]Y. Yang, A. Purwarb, and M. H. White, Solid-State Electron. **43**, 2025 (1999).